Acta of Bioengineering and Biomechanics
Vol. 17, No. 2, 2015

Original paper
DOI: 10.5277/ABB-00140-2014-02

The study of physicochemical properties of stabilizing plates removed from the body after treatment of pectus excavatum

ANITA KAJZER[1]*, WOJCIECH KAJZER[1], JÓZEF DZIELICKI[2], DAWID MATEJCZYK[1]

[1] Department of Biomaterials and Medical Devices Engineering, Faculty of Biomedical Engineering, Silesian University of Technology, Zabrze, Poland.
[2] Medical University of Silesia, School of Medicine in Katowice, Katowice, Poland.

This paper presents the results of a physicochemical surface study and clinical observation of a new generation of plates for the treatment of pectus excavatum. Analysis of the data allowed us to investigate the effect of implant design and condition of their surface on the results of treatment of pectus excavatum. In the study, we performed an analysis of clinical data, obtained after a suitable period of treatment with the use of implants, as well as a study of physicochemical properties of stabilizing plates after their removal from the body. Surface roughness, the surface wettability and corrosion resistance were measured, and the results were compared with clinical observations. When removing the plates we found only slight inflammatory-periosteal reactions around the wire fixing transverse stabilizing plates to the ribs and locking the base plate correcting the distortion. The corrective plates did not shift or rotate during the entire treatment period, giving an optimal, oval and natural shape of the chest. The obtained values of the parameters investigated indicate that the reduction in resistance to pitting corrosion occurred in the areas where laser marking was made to identify the plate. The remaining plates, in spite of mechanical damage of the surface, were characterized by good corrosion resistance, a fact which is confirmed by the results of clinical evaluation.

Key words: *stabilizing plate, corrosion resistance, clinical assessment*

1. Introduction

Malformation of the anterior chest wall causes a number of cardiovascular disorders. Compression of the right and left ventricle can lead to hemodynamic disorders and cardiac silhouette shift to the left as well as twisting of its axis and hinders the flow of blood from the lungs to the left atrium. The left shift of the heart is also linked with exposing the right cavity and a change of cardiac silhouette, which becomes similar to a mitral heart. The most common childhood asymptotic defect is a pectus excavatum. A small degree of distortion may for many years give no clinical symptoms. Only a significant degree of deformation causes cardiovascular and/or respiratory system symptoms. During puberty, the clinical symptoms usually manifest themselves as: deterioration in exercise tolerance, exertional dyspnoea, palpitations, dizziness, fainting and coughing. In the later period abnormal ventilation and perfusion with local hypoxemia appear [4], [6], [20].

The most commonly used treatments for pectus excavatum may include the Nuss method. The experience gathered and literature data allowed establishing a number of adverse events associated with the surgical Nuss technique [2], [3], [7], [12]. Among 690 patients operated on between the ages of 3 to 31 years old the following were distinguished: severe pain due to compression of the ribs by plates supported at only

* Corresponding author: Anita Kajzer, Department of Biomaterials and Medical Devices Engineering, Faculty of Biomedical Engineering, Silesian University of Technology, ul. Roosevelta 40, 41-800 Zabrze, Poland. Tel: +48 32 277 74 22, e-mail: anita.kajzer@polsl.pl

Received: July 25th, 2014
Accepted for publication: August 25th, 2014

two points and movement of the plates during breathing, plate rotation despite the various blocking protective measures or large periosteal rib reaction due to partial mobility of the plate and the destruction of the ribs in the contact zone of the plates with ribs. Therefore, Dzielicki proposed a modified method with elements of the Nuss technique. Achieving these objectives required the development of a new structural model of plate stabilizers allowing their controlled fastening to the ribs. Development of a new or modified form of the implant and the tools used for its attachment require research with application of computational mechanics methods [1], [11], [15], [22] in order to determine the biomechanical characteristics of the system under consideration. Therefore, the solution to this problem required numerical analysis [9] and preclinical experimental studies carried out in the swine chest–stabilizer plate system [8]. Obtaining positive results formed the basis for the development of our own diagnostic procedures and the modelling of procedures using minimally invasive methods for surgical treatment of pectus excavatum, mainly by changing the location and method of attachment of the plates with the cross-beams which resulted in a favourable distribution of forces acting being applied to the deformed chest. Therefore, taking into account the possibility of using minimally invasive surgical techniques and minimization of costs, the Centre of Biomedical Engineering, Silesian University of Technology developed a range of stabilizer plates and surgical instruments whose production was implemented in BHH Mikromed in Dąbrowa Górnicza.

These tests are a continuation of the issue concerning development of the modified form of plate implant for stabilization of malformations of the anterior chest wall presented in earlier papers of the authors [8]–[10].

2. Material and methods

2.1. Clinical evaluation

From October 20, 2010 to April 12, 2013 under the project titled "A new method of surgical treatment of the anterior chest wall malformations", stabilization of pectus carinatum and pectus excavatum was carried out within the terms of clinical evaluation with plates using a modified method of fixation. The additionally applied cross-bars, fixed to the ribs with wire, constituted an important factor contributing improved stabilization plate during implantation. The main corrective plate and the cross-bar had grooves to allow locking the plate with screws after achieving the forced oval and optimal shape of the chest. Such fixing prevented and eliminated the rotation of the plate, its movement and friction against the ribs. Precisely this mobility, typical of the Nuss technique, caused considerable pain and a periosteal reaction. Patients aged 16–22 years old underwent treatment. Depending on the degree of malformation, one or two plates were implanted. The implants were removed after achieving a stable, anatomical curvature of the thorax and the ribs growing during that time obtaining "shape memory". Depending on the degree of defect, the plates were removed a year (pectus carinatum malformations) up to 2 years and above (pectus excavatum) after implantation. 48 corrections of pectus excavatum and 15 corrections of pectus carinatum were performed until 30.06.2014. The exemplary images of malformations before and after surgery are shown in Fig. 1. Considering the fact that stabilization requires adequate time, we selected 4 plates removed from the patients' bodies for evaluation of physicochemical properties. These studies are complementary to the studies conducted by the authors on the plates after a specific time of implantation.

Fig. 1. The exemplary images of pectus excavatum: (a) before, (b), (c) after surgery

2.2. The study of physicochemical properties

Tests were carried out on plates of modified construction made of stainless Cr-Ni-Mo steel of a chemical composition and mechanical properties consistent with the recommendations of the ISO 5832-1 standard removed from the body: two plates after 20 months time and two 25 months after implantation, Fig. 2. The plates were subsequently cut into samples using a Bakelite disc with ceramic abradant (Al_2O_3), constituting the equipment of a Discotom-6 mechanical cutter manufactured by Struers. Water cooling was applied during cutting. This prevented overheating of the samples, which could lead to local changes in their structure. The material for testing was divided into three groups: the first sample contained surface defects in the form of numerous scratches, the second contained samples with undamaged surface, while the third group contained samples with engraving on the surface made for identification. The following were performed during the study: macroscopic surface assessment, roughness and surface wettability measurement and the test of resistance to pitting corrosion.

Evaluation of the surface was carried out using a SteREO Discovery V8 stereoscopic microscope manufactured by Zeiss with AxioVision software. Roughness measurement was made using a Surtronic 3+ contact profilographometer from Taylor Hobson. The Ra parameter was determined – the arithmetic average of profile ordinates according to the PN-EN ISO 4287 standard recommendations. To determine the wettability of the surface on the selected samples we analyzed contact angles and surface energy (SEP) with the Owens–Wendt method. Contact angle measurements were performed using two liquids: distilled water (θw) (manufactured by Poch S.A.) and diiodomethane (θw) (manufactured by Merck Sp. z o.o.). Measurement of liquid drops and diiodomethane deposited onto surfaces of the specimens was made at room temperature on a test bench consisting of a SURFTENS UNIVERSAL manual goniometer manufactured by OEG and computer with Surftens 4.5 software for the analysis of the recorded drops' image. 5 drops of distilled water and diiodomethane were applied onto the surface of each sample, each with a capacity of 1.5 µl. The measurement began 20 seconds after the application of the drops. The duration of a single measurement was 60 seconds with a sampling rate of 1 Hz. Next, the determined values of contact angles θ and surface energy were presented as mean values with standard deviation. The value of surface energies (SEP) and their components assumed for calculation: polar and dispersive, are given in Table 1.

The last stage of the analysis consisted in testing the resistance to pitting corrosion of the samples selected on the basis of macroscopic evaluation, from the areas with visible surface damage (the first group) occurring in places of laser marking (third group) and for comparison in the areas without any mechanical damage (second group). The study was performed by recording potentiodynamic polarization curves according to PN-EN ISO 10993-15 standard recommendations. The measuring set consisted of a VoltaLab PGP201 potentiostat, reference electrode (NEK KP-113 saturated calomel electrode), the auxiliary electrode (platinum electrode type PtP-201), anode (the test sample) and

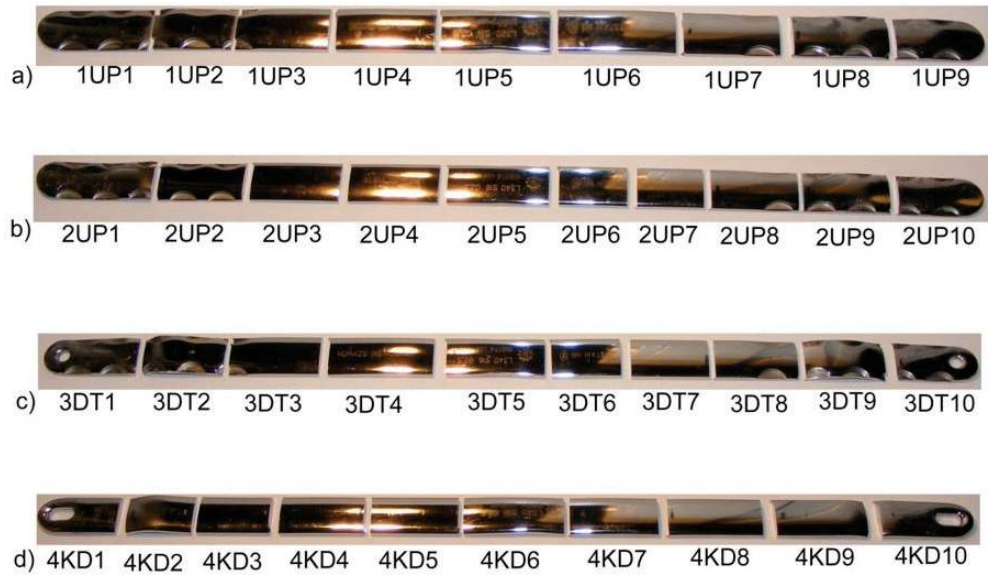

Fig. 2. Marking of test samples

a PC with VoltaMaster 4 software. Prior to testing, the surfaces of all samples were cleaned with 96% ethanol using a SONICA 1200M ultrasonic bath for $t = 6$ min. Corrosion tests began with determination of the potential of opening E_{ocp} in currentless conditions. Polarization curves were recorded from the starting potential value $E = E_{ocp} - 100$ mV. The change of potential occurred in the anode direction at a rate of 1 mV/s. After achieving the anodic current density of 1 mA/cm^2 the direction of polarization was changed. On the basis of the curves obtained, corrosion potential E_{corr}, the transpassivation potential E_{tr} as well as breakdown E_{np} and repassivation E_{cp} were determined and, using the Stern method, polarization resistance value R_p.

Table 1. The values of SEP and their individual components for measurement liquids

Type of liquid	Polar component γ_s^p mJ/m^2	Dispersion component γ_s^d mJ/m^2
Distilled water	51.0	21.8
Diiodomethane	6.7	44.1

3. Results

Based on the results of clinical evaluation and the studies conducted assessment of stability and evaluation of physicochemical properties of the selected plates were performed.

3.1. The results of clinical evaluation

The application of panels longer by about 3 cm on each side compared to those used in the Nuss technique and structural solution allowing for the possibility of firm locking of the support plate with the cross-bars made it possible to form an oval shape regardless of whether the deformation was symmetrical, unsymmetrical, or flat. The method of locking enabled stable retaining of the shape formed during the operation for the entire period of treatment. Stable locking of carrier plates and their proper adhesion to the ribs changed the size and distribution of clamping forces. The clamping forces were not concentrated at two points on the ribs, as in the Nuss method, but at four attachment zones of the stabilizing plates which reduced the pressure forces and eliminated movement of the plates. The cosmetic effect immediately after surgery in all patients was very good. In 4 patients, from whom the plate was removed, a very good cosmetic result remained permanent. There was no periosteal reaction – except one – in which earlier loosening of the wire loop occurred, causing increased friction of the plates against the rib periosteum. The plates were removed after about two years of implantation. The amount of analgesics the patients needed was minimal, and there was no need to insert analgesic catheters into the pleural cavity epidurally.

3.2. The results of physicochemical properties

On the basis of observations with a stereoscopic microscope, it was found that in most of the analyzed areas on the external surfaces of the plates, there are numerous instances of mechanical damage in the form of scratches of varying depth and width (the first group). These may have occurred during the preoperative modelling of the plates to the anatomical curvature of the chest, as well as at the time of their removal, Fig. 3. In contrast, the inner surfaces, which

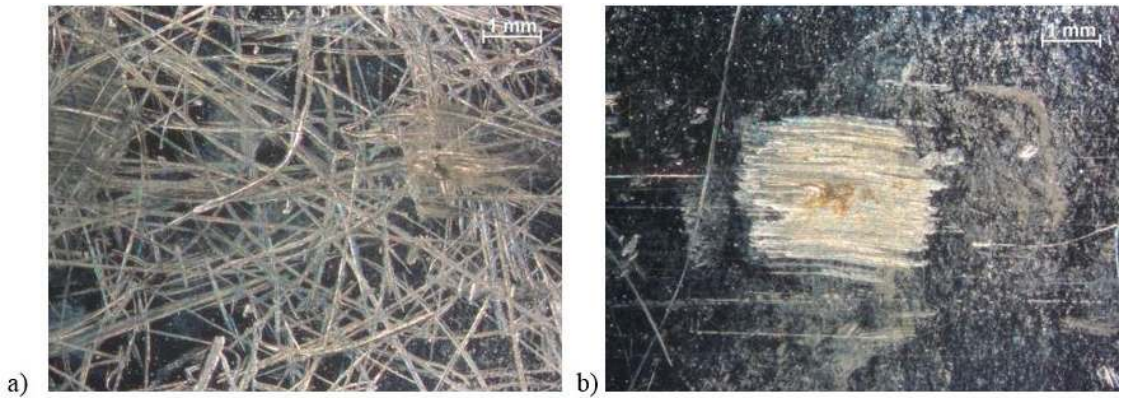

Fig. 3. Example of mechanical damage to the outer surface of the plates: (a) 2UP, (b) 4kD, stereoscopic microscope, magnification 10×

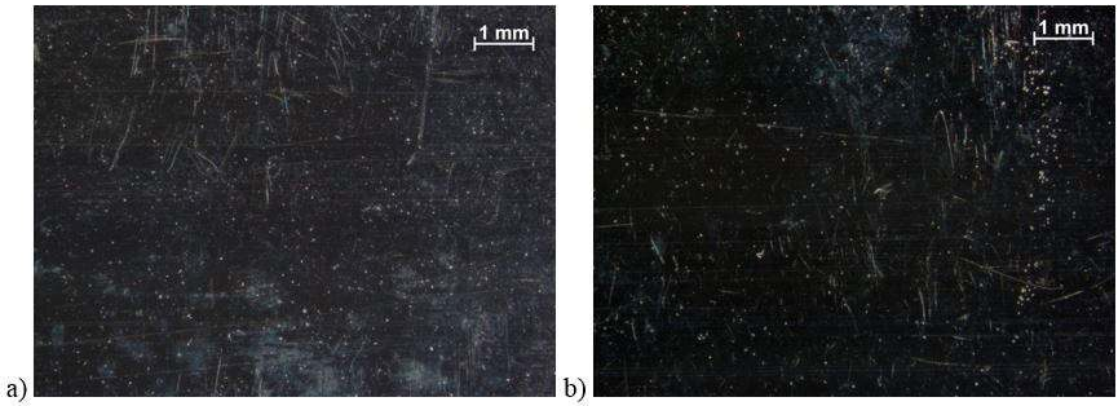

Fig. 4. Examples of mechanical damage to the inner surface of the plates:
(a) 1UP, (b) 4kD, stereoscopic microscope, magnification 10×

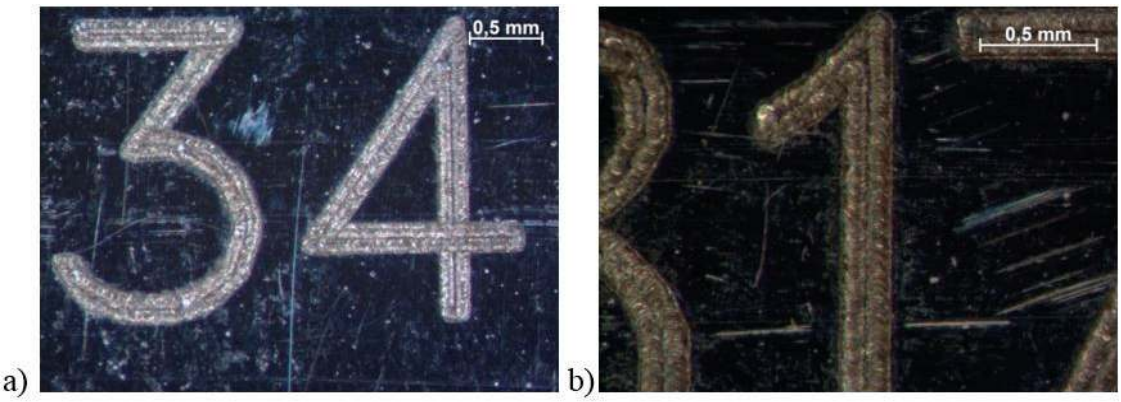

Fig. 5. Example of engraving in the central part of the plate:
(a) 3DT5, magnification 25×, (b) 2UP5, magnification 40×, stereoscopic microscope

were represented by the samples of the second group, were characterized by a mirror polish with no apparent mechanical defects, Fig. 4. Engraving was made in the middle part, which enabled identification of each of the implanted plates (third group), Fig. 5.

Deep scratches and engraving on the surface of the plates influenced the increase of Ra parameter, Table 2. It can be seen that on the inner surfaces and the panel areas without mechanical damage the Ra parameter value varied from 0.04 μm to 0.09 μm compared to a maximum of Ra = 0.85 μm for the numerous surface defects. These samples were collected from the end portions of the plates and are characterized by numerous surface scratches made while bending the implant with the use of tools to the anatomical curvature to the chest before implantation, and then removing it. An increase of the surface roughness Ra to a value of 0.74 μm was also observed in the central portion in the areas where the plates were marked for identification.

Next, surface wettability was tested on the selected samples. On the basis of these results it was found that all the analyzed plate surfaces are characterized by hydrophilic properties of low wettability. The test results, the surface wettability and the surface energy are shown in Table 3.

The highest contact angle values of the samples being tested were obtained from plate 3DT7 (θ = 81.95°). Other samples, 1UP6, 2UP8 and 4KD8, representing a particular plate, acquired respectively the mean value of the contact angle θ = 76.44°, θ = 76.75° and θ = 79.12°. An exemplary photograph of the sample of distilled water and a drop of diiodomethane applied to the outer surface of the plate is shown in Fig. 6. On the other hand, the mean values of θ for the contact angle of diiodomethane (Table 3) were similar in sequence to plates 1, 2, 3 and 4 and were as follows: θ = 58.91°, θ = 56.51°, θ = 56.28°, θ = 57.23°. Contact angle values obtained during the test using distilled water and then diiodomethane constituted the basis for further studies of the surface energy. As a result, the surface energy values γS were obtained. For samples from plates 1, 2, 3 and 4, they were close to each other and were 31.44 mJ/m^2, 32.22 mJ/m^2, 31.08 mJ/m^2 and 31.24 mJ/m^2, respectively.

Table 2. Test results of surface roughness

Plate name	Plate 1 UP								
Number of sample	1UP1	1UP2	1UP3	1UP4	1UP5	1UP6	1UP7	1UP8	1UP9
Surface roughness Ra, μm	0.13	0.04	0.05	0.60	0.11	0.14	0.05	0.33	0.50
Standard deviation, μm	±0.01	0.00	0.00	±0.01	±0.03	±0.01	±0.01	±0.06	0.00
Notes	Surface: 1UP1, 1UP8 and 1UP9 – with numerous scratches, 1UP2 – no scratches, 1UP3 and 1UP7 – internal, 1UP4, 1UP5 and 1UP6 – engraved								
Plate name	Plate 2 UP									
Number of sample	2UP1	2UP2	2UP3	2UP4	2UP5	2UP6	2UP7	2UP8	2UP9	2UP10
Surface roughness Ra, μm	0.85	0.07	0.18	0.51	0.51	0.63	0.14	0.16	0.11	0.39
Standard deviation, μm	±0.03	±0.01	0.00	±0.09	±0.02	±0.03	0.00	0.00	±0.01	±0.03
Notes	Surface: 2UP1 – with numerous scratches, 2UP2, 2UP8, 2UP9 and 2UP10 – with a few scratches, 2UP3 and 2UP7 – internal, 2UP4, 2UP5 and 2UP6 – engraved									
Plate name	Plate 3 DT									
Number of sample	3DT1	3DT2	3DT3	3DT4	3DT5	3DT6	3DT7	3DT8	3DT9	3DT10
Surface roughness Ra, μm	0.15	0.08	0.15	0.74	0.67	0.35	0.05	0.29	0.35	0.19
Standard deviation, μm	±0.01	±0.03	±0.06	±0.02	±0.08	±0.01	±0.01	±0.03	±0.02	±0.08
Notes	Surface: 3DT1, 3DT10 – with numerous scratches, 3DT2 – deformed by bending, 3DT3, 3DT8 – internal, 3DT4, 3DT5, 3DT6 – engraved, 3DT7 – the study of corrosion resistance, 3DT9 – with a few scratches									
Plate name	Plate 4 KD									
Number of sample	4KD1	4KD2	4KD3	4KD4	4KD5	4KD6	4KD7	4KD8	4KD9	4KD10
Surface roughness Ra, μm	0.19	0.66	0.09	0.09	0.37	0.74	0.25	0.09	0.10	0.87
Standard deviation, μm	±0.01	±0.02	±0.01	±0.01	±0.01	0.00	±0.01	0.01	0.00	±0.03
Notes	Surface: 4KD1, 4KD10 – with numerous scratches, 4KD2 – deformed by bending, 4KD3, 4KD4, 4KD7 – internal, 4KD5, 4KD8, 4KD9 – with a few scratches, 4KD6 – engraved									

Table 3. Results of the surface energy calculated on the basis of contact angle measurements – OWRK method

Number of sample	Distilled water Contact angle, °	Diiodomethane Contact angle, °	Polar component γ_s^p, mJ/m^2	dispersion component γ_s^d, mJ/m^2	Surface energy γ^S, mJ/m^2
1UP6	76.44 ± 3.0	58.91 ± 1.2	11.26	20.18	31.44
2UP8	76.75 ± 1.7	56.51 ± 1.7	10.24	21.98	32.22
3DT7	81.95 ± 0.9	56.28 ± 1.6	6.65	24.43	31.08
4KD8	79.12 ± 2.6	57.23 ± 0.5	8.76	22.48	31.24

Following the analysis of surface wettability, studies of resistance to pitting corrosion were performed. Examples of test results in the form of conventional and logarithmic polarization curves are shown in Fig. 7.

Characteristic parameters, whose values are shown in Table 4, were determined on the basis of the curves obtained.

The values of the recorded potentials confirm the macroscopic observations of the surface. For the

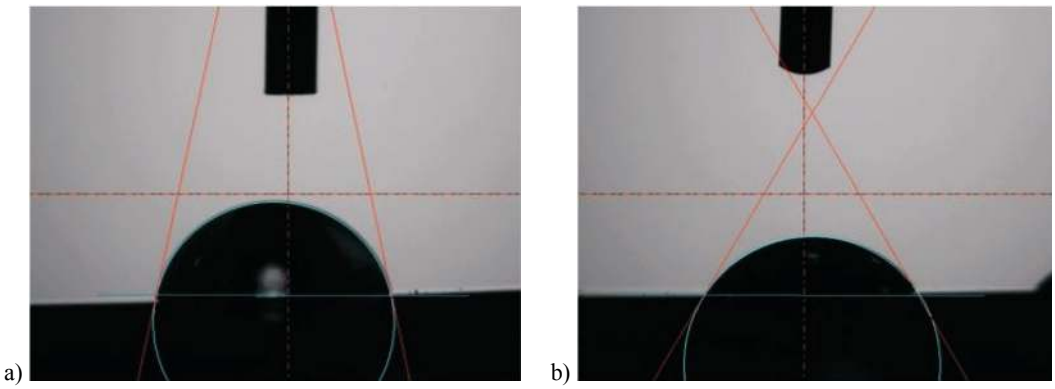

Fig. 6. Sample of drops: (a) distilled water, (b) diiodomethane deposited on the sample surface

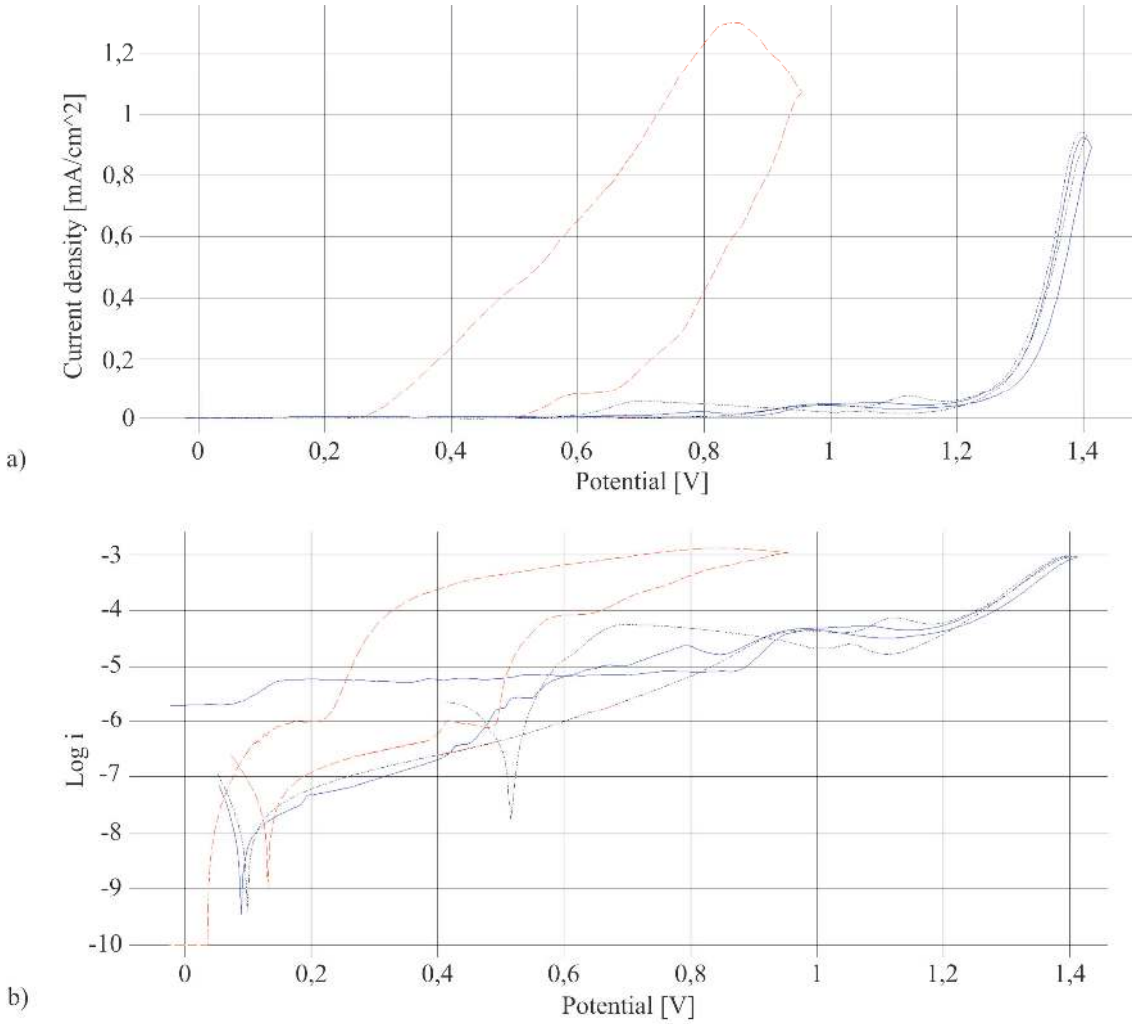

Fig. 7. Examples of polarization curves: (a) classical chart, (b) logarithmic graph: first group – solid line, second group – line dot-dash, third group – line dash-dash

surface of the plates which were laser marked (samples of the third group) we observed hysteresis loop, demonstrating the development of pitting corrosion. For these samples the breakdown potential was recorded, which varied from E_{np} = 768 mV, up to E_{np} = 1130 mV, repassivation potential E_{cp} from 19 mV up to 141 mV, with the corrosion potential E_{corr} from 68 mV up to 141 mV and polarization resistance R_p from 423 kOhm·cm^2 up to 1180 kOhm·cm^2. For the samples from the first and second groups a transpassivation potential was determined that ranged from E_{tr} = 1265 mV to E_{tr} = 1307 mV, the corrosion poten-

Table 4. Results of resistance to pitting corrosion tests of the analyzed plates

Name	Plate 1 UP					Plate 2 UP				
Number	1UP1	1UP2	1UP3	1UP4	1UP7	2UP1	2UP2	2UP3	2UP4	2UP5
Breakdown potential E_{np} [mV]	–	–	–	+768	–	–	–	–	+1103	+1130
Repassivation potential E_{cp} [mV]	–	–	–	+86	–	–	–	–	+141	+68
Transpassivation potential E_{tr} [mV]	+1302	+1286	+1306	–	+1298	+1284	+1300	+1290	–	–
Corrosion potential E_{corr} [mV]	+90	–108	+119	+141	+99	+148	+38	+97	+124	+121
Polarization resistance R_p [kOhm·cm^2]	2000	556	912	494	1440	270	1480	1160	1160	1070
Name	Plate 3 DT					Plate 4 KD				
Number	3DT1	3DT2	3DT3	3DT4	3DT5	4KD1	4KD2	4KD3	4KD4	4KD6
Breakdown potential E_{np} [mV]	–	–	–	+814	+814	+1148	–	–	–	+1062
Repassivation potential E_{cp} [mV]	–	–	–	+19	+35	+66	–	–	–	+31
Transpassivation potential E_{tr} [mV]	+1266	+1287	+1265	–	–	–	+1316	+1307	+1304	–
Corrosion potential E_{corr} [mV]	+110	+114	+101	+115	+114	+152	+133	+113	+126	+68
Polarization resistance R_p [kOhm·cm^2]	719	668	586	741	423	962	732	817	760	1180

tial E_{corr} from +148 mV up to –108 mV, while the polarization resistance R_p varied from 270 kOhm·cm^2 to 2000 kOhm·cm^2. These values indicate a good resistance to pitting corrosion of the analyzed plate areas.

Fig. 8. Examples of pitting at the site of the implant marking

The resulting reduced breakdown potential for the samples of the third group confirms the observations under the stereoscopic microscope. Pits were found in the areas in which the implant marking was performed, Fig. 8. Detailed analysis of the results of sample testing, which were marked using a laser technique, showed the occurrence of the breakdown potential and corrosion defects, which indicates a permanent interruption of the passive layer, which is not subject to repassivation in the tissue environment.

4. Discussion

Biomaterials used for plates for the treatment of pectus excavatum must meet certain normative requirements so that they do not endanger the health and life of the patient when implanted into the body [13], [19].

One of the main criteria for the evaluation of the implant is its resistance to corrosion and biotolerance in the body fluids environment, which is related to physicochemical properties of the surface. The highest average values of Ra parameter to the surfaces of the samples were obtained from the first and third groups. These samples were cut from plate areas previously bent to the correct curvature of the chest by the instruments and the areas in which laser marking was made. On the other hand, the lowest roughness values were measured for the surfaces of the samples from

the second group on the inner side of the plates and external surfaces containing few or no scratches, Table 2. The condition of the samples' surface had an impact on the resistance of stabilizers to pitting corrosion. Detailed analysis of the results of sample testing with laser marking showed a reduction of breakdown potential and corrosion defects, which indicates a permanent interruption of the passive layer, which is not subject to repassivation in the tissue environment. The potentiodynamic curves obtained for them are characterized by the presence of the characteristic hysteresis loop demonstrating the initiation of corrosion processes. Therefore, the authors suggest carrying out the marking on the surface of the implant before formation of the passive film protecting the implant body against the body fluids environment. However, the occurrence of mechanical damage in the form of surface cracks does not affect the reduction of corrosion resistance which may result from an auto-passivation in the tissue environment. This indicates the presence of transpassivation potential and lack of development of corrosion pits, as confirmed by the macroscopic observation of surface samples.

The analysis of the nature of the surface layer allows the behaviour of organic cells to be evaluated in the presence of surface layer material. The resulting mean values of contact angle indicate that the plates being tested have a hydrophilic surface, but poorly wettable. Referring to the work of authors [5], [14], [16], [21] it can be concluded that the more hydrophobic the surface of the material, the more proteins adsorbed to the surface. Conversely, the more hydrophilic the surface, the more conformational changes in the adsorbed proteins. Low protein adsorption to the surface of the biomaterial is desired because it reduces blood clotting. In turn, the surface energy can be used as an indicator of whether the cell adhesion to the surface of the biomaterial occurs. Based on this, it can be concluded that if the plate surface is hydrophilic, conformational changes of proteins of the body may occur, which may contribute to the formation of blood clots; however, the surface is poorly wetted, which greatly reduces the adsorption of proteins and the possibility of initiating corrosion processes on the surface. The energy value of the analyzed surface stabilizers indicates their athrombogenicity, which eliminates the overgrowth of bone tissue to the surface. The obtained results of wettability and corrosion resistance of the plates were confirmed by clinical results. The plates with a modified design provided very good treatment results. After removing them from the body, no tissues adsorbed to the surface have been observed. Moreover, patients treated with the new stabilizer generation felt minimal pain after implantation, which was caused by the change of distribution of pressure generated by the plate. On the other hand, the minimal periosteal-inflammatory reactions could have been caused by the formation of a "cell" in the wire-plate system upon fixing of the plate to the ribs with a cross-bar following the occurrence of crevice corrosion [17], [18]. The obtained results allow us to conclude that the use of lockable plates is a new, highly effective method of treating a malformed chest.

Acknowledgements

The work was financed from research project no 4159/B/T02/2010/38.

References

[1] BASIAGA M., PASZENDA Z., SZEWCZENKO J., KACZMAREK M., *Influence of surgical drills wear on thermal process generated in bones*, Acta Bioeng. Biomech., 2013 15(4), 21–29.

[2] BOHOSIEWICZ J., KUDELA G., KOSZUTSKI T., *Results of Nuss procedures for the correction of pectus excavatum*, Eur. J. Pediatr. Surg., 2005, 15(1), 6–10.

[3] DZIELICKI J., KORLACKI W., JANICKA I., DZIELICKA E., *Difficulties and limitations in minimally invasive repair of pectus excavatum – 6 years experiences with Nuss technique*, Eur. J. Cardiothorac. Surg., 2006, 30, 801–804.

[4] FONKALSRUD E.W., *Current management of pectus excavatum*, World J. Surg., 2003, 27, 502–508.

[5] GODDARD J.M., HOTCHKISS J.H., *Polymer surface modification for the attachment of bioactive compounds*, Prog. Polym. Sci., 2007, 32, 698–725.

[6] HALLER J.A., COLOMBANI P.M., HUMPHRIES C.T., AZIZKHAN R.G., LOUGHLIN G.M., *Chest wall constriction after too extensive and too early operations for pectus excavatum*, Ann. Thorac. Surg., 1996, 61, 1618–1625.

[7] JAROSZEWSKI D., NOTRICA D., MCMAHON L., STEIDLEY D.E., DESCHAMPS C., *Current management of pectus excavatum: a review and update of therapy and treatment recommendations*, JABFM, 2010, 23, 230–239.

[8] KAJZER A., KAJZER W., GZIK-ZROZKA B., WOLAŃSKI W., JANICKA I., DZIELICKI J., *Experimental biomechanical assessment of plate stabilizers for treatment of pectus excavatum*, Acta Bioeng. Biomech., 2013, 15(3), 113–121.

[9] KAJZER W., KAJZER A., GZIK-ZROSKA B., WOLAŃSKI W., JANICKA I., DZIELICKI J., *Comparison of Numerical and Experimental Analysis of Plates Used in Treatment of Anterior Surface Deformity of Chest*, Information Technologies in Biomedicine, Springer-Verlag, Berlin–Heidelberg, 2012, 319–330.

[10] KAJZER W., KAJZER A., *Badania potencjodynamiczne i impedancyjne implantów do leczenia zniekształceń przedniej ściany klatki piersiowej*, Przegląd Elektrotechniczny, 2013, 12, 275–279.

[11] KAJZER W., KRAUZE A., KACZMAREK M., MARCINIAK J., *FEM Analysis of the Expandable Intramedullary Nail*,

Information Technologies in Biomedicine, ASC, Vol. 47, Springer-Verlag, Berlin–Heidelberg, 2008, 537–544.

[12] KELLY R.E., SHAMBERGER R.C., MELLINS R.B., *Prospective multicenter study of surgical correction of pectus excavatum: Design, perioperative complications, pain, and baseline pulmonary function facilitated by internet-based data collection*, J. Am. Coll. Surg., 2007, 205, 205–216.

[13] KIEL M., SZEWCZENKO J., MARCINIAK J., NOWIŃSKA K., *Electrochemical properties of Ti-6Al-4V ELI alloy after anodization*, Information Technologies in Biomedicine, Springer-Verlag, Berlin–Heidelberg, 2012, 369–378.

[14] KIM M.S., KHANG G., LEE H.B., *Gradient polymer surfaces for biomedical applications*, Prog. Polym. Sci., 2008, 33(1), 138–164.

[15] KRAUZE A., MARCINIAK J., *Biomechanical analysis of a femur-intramedullary nails system in children*, Danubia-Adria Symposium on Experimental Methods and Solid Mechanics, 22nd DAS – 2005, Parma, 2005, 80–81.

[16] LIBER-KNEĆ A., ŁAGAN S., *Zastosowanie pomiarów kąta zwilżania i swobodnej energii powierzchniowej do charakterystyki powierzchni polimerów wykorzystywanych w medycynie*, Polim. Med., 2014, 44, 29–37.

[17] MANIVASAGAM G., DHINASEKARAN D., RAJAMANICKAM A., *Biomedical Implants: Corrosion and its Prevention – A Review*, Recent Patents on Corrosion Science, 2010, 2, 40–54.

[18] MUDALI U., SRIDHAR T.M., RAJ B., *Corrosion of bio implants*, Sādhanā, India, 28 (3,4), 601–637.

[19] WALKE W., PRZONDZIONO J., *Influence of hardening and surface modification of endourological wires on corrosion resistance*, Acta Bioeng. Biomech., 2012, 14(3), 93–99.

[20] WILLITAL G.H., SAXENA A.K., SCHUTZE U., RICHTER W., *Chest deformities: a proposal for a classification*, World J. Pediatr., 2011, 7, 118–23.

[21] XU L.C., *Effect of surface wettability and contact time on protein adhesion to biomaterial surfaces*. Biomaterials, 2007, 28, 3273–3283.

[22] ZIĘBOWICZ A., KAJZER A., KAJZER W., MARCINIAK J., *Metatarsal osteotomy using double-threaded screws – biomechanical analysis*, Information Technologies in Biomedicine, Springer-Verlag, Berlin–Heidelberg, 2010, 465–472.